# Self-Assembled Superlattice by Spinodal Decomposition during Growth

I. Daruka[1] and J. Tersoff[2]

[1]Department of Theoretical Physics, University of Debrecen, P.O. Box 5, H-4010 Debrecen, Hungary
[2]IBM Research Division, T. J. Watson Research Center, P.O. Box 218, Yorktown Heights, New York 10598, USA

(Received 3 January 2005; published 12 August 2005)

We examine the dynamics of alloy growth by vapor deposition and bulk diffusion, predicting a new type of self-organized growth. When material is deposited at a composition unstable against spinodal decomposition, we find three distinct regimes depending on growth rate. Intermediate growth rates lead to spontaneous formation of a superlattice with layers parallel to the surface. Slow growth leads to more complex three-dimensional decomposition. For fast growth, the alloy composition remains uniform near the surface, with a composition wave propagating up from the interface.

DOI: 10.1103/PhysRevLett.95.076102 PACS numbers: 81.16.Dn, 68.35.Fx, 68.65.Cd, 81.16.Rf

There is intense interest in self-assembly of nanostructured materials. Besides the inherent interest of the physical processes involved, self-assembly holds promise for technological applications. Recent years have witnessed increasing success in the controlled self-assembly of quantum dots, quantum wires, and superlattices [1–7].

Here we consider spinodal decomposition [8] as a mechanism for structure formation. Spinodal decomposition in an alloy $A_xB_{1-x}$ is the common tendency to phase separate into $A$-rich and $B$-rich phases. Most work has focused on semiconductor growth at relatively low temperature, where the evolution occurs primarily by surface diffusion rather than bulk diffusion. In this regime, spinodal decomposition is expected to lead to composition modulation perpendicular to the growth direction [9,10] (unless growth is by step flow [11,12]). We consider instead a very different regime, where the evolution is dominated by bulk diffusion and surface diffusion can be neglected relative to bulk diffusion. We also consider what systems are good candidates for showing this behavior.

We find three distinct regimes of dynamical behavior, depending upon the growth rate. Most interestingly, the regime of intermediate growth rate leads to spontaneous formation of a superlattice, with layers parallel to the surface, as shown in Fig. 1(b). A linear stability analysis shows that this planar superlattice formation is dynamically stable. In this regime, the superlattice period is comparable to the equilibrium domain boundary width [8]. Thus the periodicity can easily be nanoscale and can be controlled by varying the deposition rate and/or temperature. This apparently represents a new mechanism for self-organized growth of nanoscale structures.

Slower growth leads to more complex three-dimensional (3D) decomposition, perhaps resembling that predicted for surface diffusion [9,10]. For faster growth, in contrast, the alloy composition remains uniform near the surface. In this case, composition modulation propagates from the substrate toward the surface [Fig. 1(a)]. This is closely analogous to the well-studied phenomenon of surface-directed spinodal decomposition [13,14], but with decomposition initiated at the substrate rather than at the surface.

In our simulations, we assume a specific though rather generic form for the free energy. (This is necessary because the usual bulk continuum equations for spinodal decomposition leave some ambiguity about the gradient term at the surface.) The enthalpy of mixing of the $A$-$B$ alloy is taken to be

$$E = \frac{1}{2}\frac{1}{V_0^2}\int c(\mathbf{r})[1 - c(\mathbf{r}')]v(\mathbf{r}, \mathbf{r}')\mathbf{dr}\mathbf{dr}', \qquad (1)$$

where $\mathbf{r}$ and $\mathbf{r}'$ denote 3D positions, $V_0$ is the atomic volume, and $c(\mathbf{r})$ is the local composition (fraction of $A$ atoms). The integral is over the solid and excludes the vacuum region. The enthalpy of mixing is described by the short-range $A$-$B$ interaction:

$$v(\mathbf{r}, \mathbf{r}') = he^{-(\mathbf{r}-\mathbf{r}')^2/R^2}, \qquad (2)$$

where $h$ is the interaction strength and $R$ is the characteristic range of the interaction. The free energy additionally includes the entropic contribution $(kT/V_0)\int[c\ln c + (1 - c)\ln(1 - c)]\mathbf{dr}$.

The specific form of $v(\mathbf{r})$ is not important, only the range and strength. The standard form for enthalpy of mixing used in regular solution theory [8], $E/N = \frac{1}{2}Hc(1 - c)$, is recovered here with $H = \pi^{3/2}V_0^{-1}R^3h$. The positive enthalpy of mixing favors decomposition, while entropy favors mixing. Entropy dominates at high $T$, while spinodal decomposition occurs for temperatures below $kT_c = \frac{1}{4}H$.

Because of the finite range of the interaction (2), large composition gradients are unfavorable. In equilibrium, the boundary between regions of different composition has a finite thickness $\lambda$, which increases with increasing temperature and diverges at $T_c$ [8]. In regular solution theory, this effect is represented by a gradient term $\frac{1}{2}m(\nabla c)^2$ in the free energy. This standard form is recovered here with $m = \pi^{3/2}hR^5/(2V_0)$.

 

From the free energy above, we calculate $\mu$, the difference in chemical potential between $A$ and $B$ atoms:

$$\mu(\mathbf{r}) = \frac{1}{V_0}\int\left[\frac{1}{2} - c(\mathbf{r}')\right]v(\mathbf{r}-\mathbf{r}')\mathbf{d}\mathbf{r}' + kT\{\ln c(\mathbf{r}) - \ln[1-c(\mathbf{r})]\}. \quad (3)$$

Since we assume that surface diffusion is negligible relative to bulk diffusion, the concentration evolves as $\partial c/\partial t = D\nabla^2\mu$, where $D$ is the mobility. The boundary condition is zero normal diffusion at the surface (and at the back surface of the substrate).

After scaling, the dimensionless evolution equation is

$$\frac{\partial c}{\partial \zeta_s} = f^{-1}\tilde{\nabla}^2\tilde{\mu}. \quad (4)$$

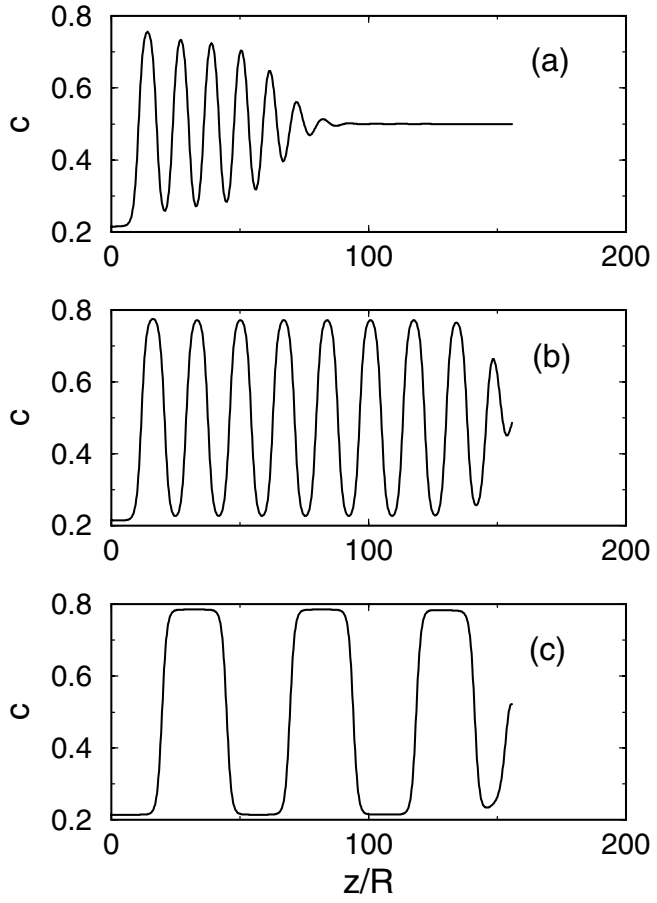


FIG. 1. Composition profiles along the growth direction for different deposition rates. The substrate is to the left, and the curves end at the growing surface on the right. The figure shows two types of composition modulations. (a) At scaled deposition rate $f = 0.25$, the composition modulations do not reach a steady state. The propagation velocity of the composition modulations is smaller than the velocity of the growing surface. Thus, the growing surface outruns the oscillations. At slower deposition rates (b) $f = 0.05$ and (c) $f = 0.006\,25$, the composition modulations reach a steady state.

Here $\zeta_s = z_s/R$, where $z_s$ is the position of the growing surface; $f = F/F_0$ is the scaled deposition rate, where $F = dz_s/dt$ is the deposition rate; and the characteristic deposition rate is $F_0 = 4kT_cD/R$. Also, $\tilde{\nabla}^2$ is the dimensionless Laplace operator, scaled by $R$. The scaled chemical potential is

$$\tilde{\mu}(\xi) = \pi^{-3/2}\int\left[\frac{1}{2} - c(\xi')\right]\exp([\xi-\xi']^2)\mathbf{d}\xi' + \frac{T}{4T_c}\{\ln c(\xi) - \ln[1-c(\xi)]\}, \quad (5)$$

with $\xi = \mathbf{r}/R$.

For the simulations reported here, we choose a deposition composition $c_{\text{dep}} = 0.5$ and temperature $T = 0.88T_c$. Then in equilibrium, the material would decompose into compositions $c_1 = 0.21$ and $c_2 = 0.79$. We choose a substrate composition equal to $c_1$. (We have also studied the cases with $c_{\text{dep}} = 0.4$ and 0.6, and the results show qualitatively the same features.) The substrate triggers spinodal decomposition with a modulation normal to the substrate, as shown in Fig. 1. We first address these one-dimensional (1D) modulations, and then examine their 3D stability.

For fast growth, we find the behavior shown in Fig. 1(a). Spinodal decomposition is initiated at the substrate, but the growing surface outruns the composition modulation. The composition remains uniform ($c = c_{\text{dep}}$) near the growing surface. We find that a composition wave propagates from the substrate toward the surface at a velocity which is independent of the growth rate. This is essentially the same phenomenon as surface-directed spinodal decomposition [13,14], except that here it is the substrate rather than the surface that initiates the decomposition.

We have determined numerically that the critical growth rate for this behavior at $c_{\text{dep}} = 0.5$ and $T = 0.88T_c$ is $f_c = 0.13$. This growth rate corresponds to the velocity at which the decomposition wave propagates in the uniform bulk.

For slower deposition rates ($f < f_c$), the composition modulations reach an oscillatory steady state, shown in Figs. 1(b) and 1(c). The wavelength and the amplitude of the composition modulations are shown in Fig. 2, plotted against the *inverse* deposition rate $f^{-1}$. Both the wavelength and the amplitude of the modulation increase with slower deposition. The composition modulation in fact corresponds closely to the equilibrium profile for a system constrained to have 1D modulation of the specified periodicity.

To understand the physical origin of the oscillations, in Fig. 3 we plot the composition profile at several successive times. Figure 3(a) shows the evolution for the same slow deposition rate as in Fig. 1(c). By the second or third time interval shown, the $B$-rich layer near the surface has reached its equilibrium composition $c = 0.21$, and the layer is simply growing thicker with time. As the deposited material decomposes, the excess $A$-rich material remains near the surface, where it forms an $A$-rich surface layer.

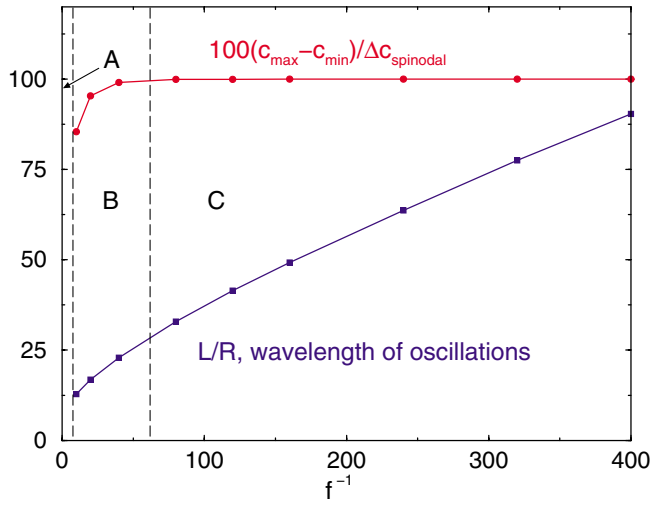


FIG. 2 (color online). The lower curve shows the wavelength $L$ of the composition modulations, in units of the interaction potential range $R$. One can see that the wavelength increases with the *inverse* deposition rate $f^{-1}$ (shown in units of $4kT_cD/R$). The upper curve shows the amplitude of composition modulations as a function of the inverse deposition rate, $f^{-1}$. The two dashed lines separate the three different growth regimes discussed in the text.

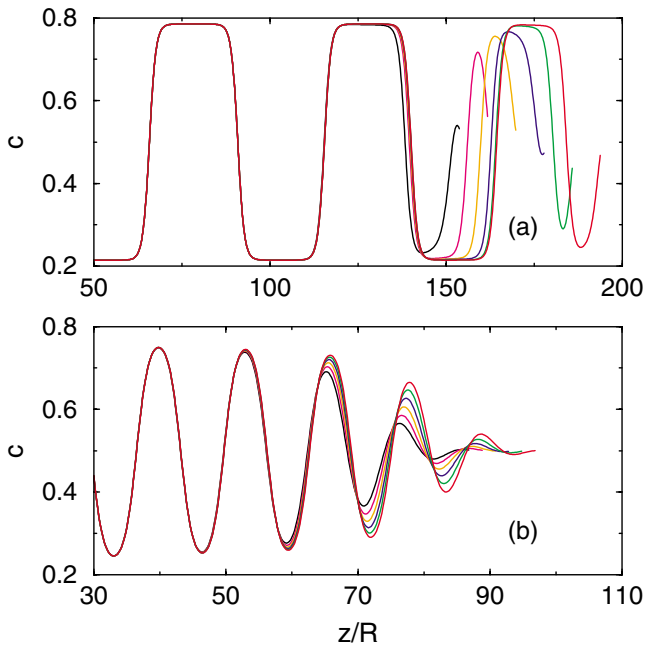


FIG. 3 (color online). Evolution of the composition profile during growth, for growth rates (a) $f = 0.006\,25$, and (b) $f = 0.1$. At each successive time, the surface has advanced, so the curve extends further to the right.

As fresh material is deposited on the surface, $B$ atoms must diffuse through the $A$ layer to the $B$ layer below. This process continues through the fourth time shown in Fig. 3(a). However, as the $A$-rich surface layer grows thicker, it becomes increasingly difficult for $B$ atoms to diffuse quickly enough to the subsurface $B$ layer. Instead, a new $B$ layer forms at the surface, at which point further growth of the subsurface $B$ layer ceases. This explains why the wavelength of the oscillation increases with decreasing growth rate: for slow growth, there is enough time for diffusion over a longer distance.

For faster deposition, the situation is more dynamic and less clear-cut. This is shown in Fig. 3(b), where we plot the composition profile at several successive times, for a rather fast deposition rate [but not quite so fast that the growing surface outruns the oscillations, as in Fig. 1(a)]. In this case, the subsurface layers do not have time to reach their final composition before a new layer forms at the surface.

(Spinodal decomposition via bulk diffusion can also give interesting 1D evolution for a heteroepitaxial film, including formation of subsurface alloy layers, even in the absence of a deposition flux. This has been studied in particular for a $B$-rich surface layer when surface segregation favors an $A$-rich layer [15].)

It is striking that, during uniform continuous deposition, the system automatically self-organizes to form a highly ordered superlattice. However, to be useful, the order must persist even in the presence of perturbations. We therefore test the dynamical stability of the self-organized superlattice growth. It is sufficient to consider the linear stability with respect to small perturbations, which can be expanded in the form

$$c(\mathbf{r}) = c(z) + c_q(z)e^{iqx}. \tag{6}$$

Since the $x$ direction can be any direction perpendicular to the growth direction $z$, this analysis determines the full 3D stability.

We use a small initial perturbation localized at the initial surface, with a wave vector $\mathbf{q}$ parallel to the surface, and amplitude $c_{q0}$. We have found that $c_q$ decays exponentially in the bulk. Thus, for the stability analysis, it is sufficient to monitor $c_q$ at the growing surface.

Figure 4 shows the calculated instability growth rate, $G = d[\ln|c_q(\zeta_s)|]/d\zeta_s$, as a function of the dimensionless wave number $qR$ for several deposition rates $f$. Because of the competition among the different length scales in our model, the behavior of the growth rate vs the wave number is complex. For $f > f_c$ (faster deposition rates) there are no stable patterns even in one spatial dimension, as discussed above and illustrated in Fig. 1(a). For deposition rates $f < f_c$, Fig. 4 indicates that the 3D stability of the 1D patterns is determined by the small $q$ (long wavelength) behavior. Even though the upper envelope of the growth rate curves has a second maximum around $qR = 0.4$, the corresponding growth rate value at this maximum is always negative; i.e., perturbations decay rather than grow.

We numerically determined the instability growth rates at long wavelength, as a function of deposition rate. We found that the system is unstable against modulations $c_q$

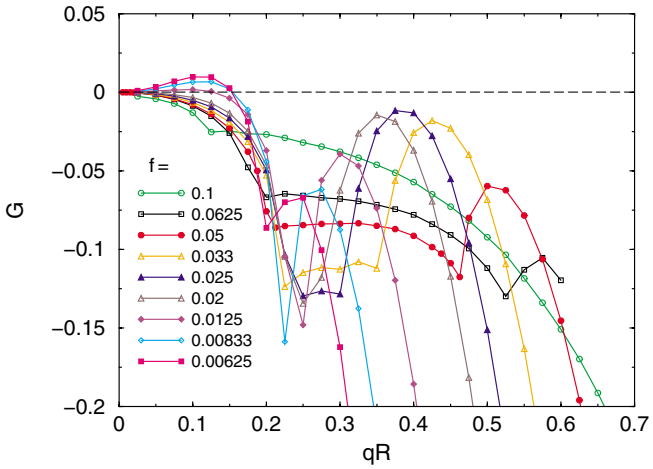


FIG. 4 (color online). Growth rate $(G = d[\ln|c_q(\zeta_s)|]/d\zeta_s)$ curves of a transverse perturbation for different deposition rates ($f$) as a function of the dimensionless wave number $qR$. Our detailed numerical investigations showed that, for intermediate deposition rates ($f_{st} = 0.016 < f < f_c = 0.13$), the 1D patterns are stable in three dimensions.

for deposition rates $f < f_{st} = 0.016$, and is stable at faster growth rates. Thus, for intermediate deposition rates $f_{st} < f < f_c$, the 1D modulations are stable in three dimensions, giving self-organized superlattice growth.

The regime for stable superlattice growth (Fig. 2) corresponds to wavelengths a few times the equilibrium boundary thickness. Thus the absence of lateral instability is probably related to the fact that the decomposition is already constrained by composition-gradient effects, and lateral decomposition would further increase the gradient.

Finally, we consider what systems and conditions are good candidates for finding self-organized superlattice growth. For bulk diffusivity $D$ and surface diffusivity $D_s$, we define a length scale $L_s = D_s/D$. For variations in $\mu$ over length scales $\gg L_s$, the response will be dominated by bulk diffusion. Variations over length scales $\ll L_s$ (in a region that includes the surface) will be dominated by surface diffusion. The gradient term effectively suppresses spinodal decomposition on length scales much below the equilibrium interface thickness $\lambda$, and the layer thickness for stable self-organized growth is also of order $\lambda$. Therefore, the assumption that bulk diffusion dominates will be valid whenever $\lambda \gg L_s$.

We can always guarantee that this condition is satisfied, by working at temperatures sufficiently close to $T_c$, where $\lambda$ becomes arbitrarily large. This requires slow growth and gives a weak modulation with a long periodicity. The modulation amplitude of the composition could be increased by postannealing at lower $T$.

To achieve shorter wavelengths and allow more rapid growth, it is desirable to find a system where the activation energy for bulk diffusion is small, relative to the growth temperature. Diffusion is a thermally activated process, and the energy barrier is reduced at the surface relative to the bulk. For semiconductors at typical growth temperatures, the activation energy is many times larger than $kT$, so the reduced energy barrier corresponds to strongly enhanced diffusivity at the surface. If the activation energy for bulk diffusion is not too much larger than $kT$, then there will not be such a strong enhancement of surface diffusivity, giving shorter $L_s$. Another approach, instead or in addition, would be to suppress surface diffusion by the use of surfactants [16].

In conclusion, we have examined the growth of a spinodally unstable system evolving by bulk diffusion. We find three distinct growth regimes, one of which corresponds to dynamically stable self-organized growth of a planar superlattice. The superlattice compositions and periodicity can be controlled, suggesting the possibility of interesting applications.

We gratefully acknowledge discussions with A.-L. Barabási. The work of I. D. was supported by the Hungarian National Scientific Fund OTKA T037212 and by the Bolyai Janos Research Foundation of the Hungarian Academy of Sciences.

[1] V. A. Shchukin and Dieter Bimberg, Rev. Mod. Phys. **71**, 1125 (1999).
[2] J. Stangl, V. Holý, and G. Bauer, Rev. Mod. Phys. **76**, 725 (2004).
[3] C. Teichert, M. G. Lagally, L. J. Peticolas, J. C. Bean, and J. Tersoff, Phys. Rev. B **53**, 16 334 (1996); J. Tersoff, C. Teichert, and M. G. Lagally, Phys. Rev. Lett. **76**, 1675 (1996).
[4] L. Bai, J. Tersoff, and Feng Liu, Phys. Rev. Lett. **92**, 225503 (2004).
[5] F. J. Himpsel, K. N. Altmann, R. Bennewitz, J. N. Crain, A. Kirakosian, J. L. Lin, and J. L. McChesney, J. Phys. Condens. Matter **13**, 11 097 (2001).
[6] P. Venezuela, J. Tersoff, J. A. Floro, E. Chason, D. M. Follstaedt, Feng Liu, and M. G. Lagally, Nature (London) **397**, 678 (1999).
[7] C. A. Wang, C. J. Vineis, and D. R. Calawa, Appl. Phys. Lett. **85**, 594 (2004); Mater. Res. Soc. Symp. Proc. **794**, T9.6.1 (2004).
[8] A. G. Khachaturyan, *Theory of Structural Transformations in Solids* (John Wiley & Sons, New York, 1983).
[9] M. Atzmon, D. A. Kessler, and D. J. Srolovitz, J. Appl. Phys. **72**, 442 (1992).
[10] F. Leonard and R. C. Desai, Phys. Rev. B **56**, 4955 (1997).
[11] A.-L. Barabási, Appl. Phys. Lett. **70**, 764 (1997).
[12] J. Tersoff, Phys. Rev. B **56**, R4394 (1997).
[13] R. A. L. Jones, L. J. Norton, E. J. Kramer, F. S. Bates, and P. Wiltzius, Phys. Rev. Lett. **66**, 1326 (1991).
[14] G. Brown and A. Chakrabarti, Phys. Rev. A **46**, 4829 (1992).
[15] J.-M. Roussel, A. Saul, G. Treglia, and B. Legrand, Phys. Rev. B **60**, 13 890 (1999); **69**, 115406 (2004).
[16] R. M. Tromp and M. C. Reuter, Phys. Rev. Lett. **68**, 954 (1992); S.-J. Kahng, J.-Y. Park, and Y. Kuk, Phys. Rev. B **60**, 16 558 (1999).